



Obrabotka metallov -

Metal Working and Material Science





Journal homepage: http://journals.nstu.ru/obrabotka_metallov







Effect of laser radiation wavelength on the structure and functional properties of TiNi alloy during UV laser treatment

Tatyana Sablina^{a,*}, Marina Kandaurova^b, Ilya Zyatikov^c, Yuriy Panchenko^d

Institute of High Current Electronics of the Siberian Branch of the Russian Academy of Sciences, 2/3 Akademicheskoy Avenue, Tomsk, 634055, Russian Federation

^a  <https://orcid.org/0000-0002-5941-5732>,  sablta@mail.ru; ^b  <https://orcid.org/0000-0003-0236-2227>,  panchenko.marina4@gmail.com;

^c  <https://orcid.org/0000-0003-3219-9299>,  zyatikov@lgl.hcei.tsc.ru; ^d  <https://orcid.org/0000-0001-8017-7268>,  yu.n.panchenko@mail.ru

ARTICLE INFO

Article history:

Received: 08 October 2025

Revised: 17 October 2025

Accepted: 31 October 2025

Available online: 15 December 2025

Keywords:

Ultraviolet laser radiation

Radiation wavelength

Surface modification

Laser treatment

Wettability

TiNi alloy

Funding

This research was carried out with support from the Russian Science Foundation grant No. 25-79-31008, <https://rscf.ru/project/25-79-31008/>.

ABSTRACT

Introduction. The widespread use of TiNi-based functional alloys in medicine requires targeted management of their surface properties, such as wettability and biocompatibility. One of the promising methods for surface modification is laser treatment, especially in the UV range of the spectrum. The efficiency of UV laser treatment is due to the high photon energy, strong absorption by metals, and the shallow depth of the thermal effect zone. **The purpose of this work** is to investigate the effect of UV laser radiation wavelength (266 and 355 nm) on the structural and phase state, chemical composition, and wettability of the TiNi alloy surface, with the goal of subsequently controlling the material's functional properties. **Materials and research methods.** TiNi surface modification was performed using a pulsed Nd:YAG laser operating at wavelengths of 266 and 355 nm in ambient air. The modified surfaces were analyzed by scanning electron microscopy with energy-dispersive spectroscopy (SEM-EDS). Microstructure, elemental composition, and phase composition were analyzed by X-ray diffraction (XRD). Wettability was estimated using the sessile drop method. The free surface energy, along with its dispersive and polar components, was then calculated from the contact angle data using the OWRK method. **Results and discussion.** UV laser treatment, varying parameters such as laser radiation wavelength and scanning speed, was found to induce changes in the morphology, elemental composition, phase composition of the surface layer of TiNi alloy samples, and their surface properties. Following UV laser treatment at wavelengths of 266 and 355 nm and low scanning speeds ($V = 200$ and $500 \mu\text{m/s}$), single microcracks or microcrack networks resulting from thermal exposure were observed on the specimen surfaces. The oxygen content on the TiNi surface increased by a factor of 5 to 18 compared to the initial state after UV laser treatment. Furthermore, the phase composition of the TiNi alloy underwent noticeable changes, with titanium oxide phases being detected on the surface after laser exposure. The higher-energy photons ($\lambda = 266$ nm) resulted in a more pronounced change in the surface morphology and properties of TiNi compared to the 355 nm radiation under identical treating conditions. UV laser treatment significantly increased the surface hydrophilicity: the contact angle decreased from $\approx 75^\circ$ in the initial state to $\approx 25^\circ$ and $\approx 11^\circ$ after treatment with 355 and 266 nm radiation wavelength, respectively. Additionally, an increase in the free surface energy of the TiNi specimens was observed, primarily due to a significant increase in the polar component.

For citation: Sablina T.Y., Kandaurova M.Yu., Zyatikov I.A., Panchenko Yu.N. Effect of laser radiation wavelength on the structure and functional properties of TiNi alloy during UV laser treatment. *Obrabotka metallov (tekhnologiya, oborudovanie, instrumenty) = Metal Working and Material Science*, 2025, vol. 27, no. 4, pp. 257–271. DOI: 10.17212/1994-6309-2025-27.4-257-271. (In Russian).

Introduction

Alloys based on titanium nickelide (TiNi) occupy an important place among functional materials due to their unique properties, such as the shape memory effect and superelasticity, which makes them attractive for use in medicine (implants, stents), the aerospace industry, and microelectronics [1–3]. However, the successful application of TiNi largely depends on its surface properties, including wettability, which affects

* Corresponding author

Sablina Tatyana Yu., Ph.D. (Engineering), Scientific associate
 Institute of High Current Electronics
 of the Siberian Branch of the Russian Academy of Sciences,
 2/3 Akademicheskoy Avenue,
 634055, Tomsk, Russian Federation
 Tel.: +7 913 843-21-78, e-mail: sablta@mail.ru

the alloy's biocompatibility and corrosion resistance [4]. Therefore, researchers' attention is focused on finding effective surface treatment methods for these alloys to improve their biofunctional properties.

Modern strategies for surface modification of functional materials include a wide range of methods, such as ion implantation [5], high-energy techniques (laser, electron beam, plasma) [6, 7], thermal and chemical treatments [8], deposition of functional coatings [9], etc. Among high-energy methods, laser treatment holds a special place due to its precision, non-contact nature, environmental friendliness, and high processing speed [6, 10]. A key advantage of laser surface modification technologies is the ability to precisely control changes in microstructure, chemical composition, and surface topography, which opens prospects for targeted control of its functional properties.

Numerous studies confirm the positive effect of laser treatment on the corrosion resistance and biocompatibility of *TiNi*-based alloys, particularly by reducing the migration of nickel ions into the physiological environment [11–15]. It was shown in [11] that treatment with an *Nd:YAG* laser ($\lambda = 1,064$ nm) improves corrosion resistance due to the formation of a protective oxide layer, although excessive melting can locally enhance nickel ion release from the *TiNi* surface. In turn, *Q. Zhang* et al. [12] demonstrated that ultrashort laser pulses not only control wettability but also create wettability gradients, which improves anti-adhesion properties and reduces the hemolytic activity of *TiNi*. Study [13] showed that texturing with femtosecond laser pulses ($\lambda = 1,028$ nm) creates hierarchical structures on the *TiNi* alloy surface, significantly improving wettability and promoting endothelialization. Other work [14] indicates that laser-induced changes in the oxide layer impart antibacterial properties to the surface, reducing *Staphylococcus aureus* adhesion. Additionally, it was found in [15] that controlling the parameters of femtosecond laser ($\lambda = 1,035$ nm) microtreatment enables achieving low surface roughness in *TiNi* powder samples, which improves biocompatibility and resistance to biocorrosion.

Nevertheless, systematic studies on the influence of laser treatment on the wettability and biocompatibility of titanium nickelide-based alloys remain limited. Despite these achievements, the task of controlling the wettability of the *TiNi* surface by laser methods is far from complete and requires in-depth research, especially for industrial implementation. At the same time, the application of ultraviolet (*UV*) laser radiation to modify the surface of *TiNi* alloy is a little-studied area. Laser radiation in the *UV* range ($\lambda = 100$ – 400 nm) has higher photon energy and stronger absorption in metals, which leads to lower penetration depth and a reduced size of the thermal effect zone compared to radiation in the visible and infrared ranges [10, 16]. In [17] we found that local exposure to *UV* laser radiation ($\lambda = 266$ nm) on stainless steel and *TiNi* alloy leads to a significant increase in surface hydrophilicity due to oxidation and an increase in the polar component of the surface free energy. *Y. Wang* and co-authors [18] have shown that exposure to nanosecond *UV* laser radiation ($\lambda = 355$ nm) makes it possible to create a controlled texture with a roughness of ≈ 5 μm on the surface of a titanium alloy, ensuring high cellular adhesion and proliferation. In [19] it was found that nanostructuring of the surface using a laser with a wavelength of $\lambda = 355$ nm improves the adhesion and proliferation of osteoblasts on the *TiNi* alloy. Thus, despite the proven effectiveness of *UV* laser treatment, there is no data in the literature on a comprehensive study of the influence of its parameters on the surface characteristics and wettability of metallic materials. Most existing works use a fixed wavelength (often 266 or 355 nm), and systematic studies varying the wavelength under controlled conditions are lacking.

The purpose of this work is to study the influence of the wavelength of *UV* laser radiation (266 and 355 nm) on the structural and phase state, chemical composition, and wettability of the *TiNi* alloy surface for subsequent control of the material's functional properties.

The objectives of the study are:

- conducting a comparative analysis of the morphology, chemical, and phase composition of the surface of *TiNi* specimens before and after *UV* laser treatment with various parameters (wavelength, scanning speed);
- estimation of the hydrophilicity degree of the surface by measuring the contact wetting angles and calculating the free surface energy with determination of dispersion and polar components of the studied *TiNi* specimens subjected to *UV* laser treatments according to different modes;
- investigating the influence of wavelength (266 and 355 nm) radiation during *UV* laser treatment on the structural and phase state and functional properties of the modified *TiNi* alloy surface.

Materials and methods of research

The specimens for investigation were 10 mm × 10 mm × 3 mm plates made of a *TiNi* alloy, grade *TN-10* (chemical composition: 50.0–51.5% *Ni*, 0.5–1.5% *Mo*, ≤0.5% *Fe*, bal. *Ti*, at. %), hereafter referred to as *TiNi*. To ensure a consistent initial surface topography for all specimens, standard surface preparation procedures were employed. All specimens were mechanically ground and subsequently subjected to final polishing using diamond pastes (*ASM* and *ASN* grades, with abrasive particle sizes ranging from 3/2 to 1/0 μm) to achieve a smooth, mirror-like surface. For final contamination removal, the specimens were ultrasonically cleaned in ethanol for 10 minutes.

The prepared surfaces of the specimens were irradiated with a pulsed *Nd:YAG* laser (*Model LS2137U, Lotis III*, Belarus) in the ultraviolet (*UV*) range. The third (355 nm) and fourth (266 nm) harmonic wavelengths of the laser radiation were used for the treatment. The laser treatment was conducted in ambient air at atmospheric pressure and room temperature (22 ± 3 °C). The main parameters of the *UV* laser treatment are summarized in Table. A schematic of the *UV* laser treatment setup and the laser scanning strategy are presented in Fig. 1.

***UV* laser treatment parameters**

Wavelength, nm (λ)	Pulse duration, ns	Pulse repetition rate, Hz	Laser spot diameter, mm (d_0)	Fluence, J/cm ² (j)	Scanning speed, μm/s (V)
266	7	10	3.5	0.22	200–5,000
355	7	10	3.5	0.22	200–5,000

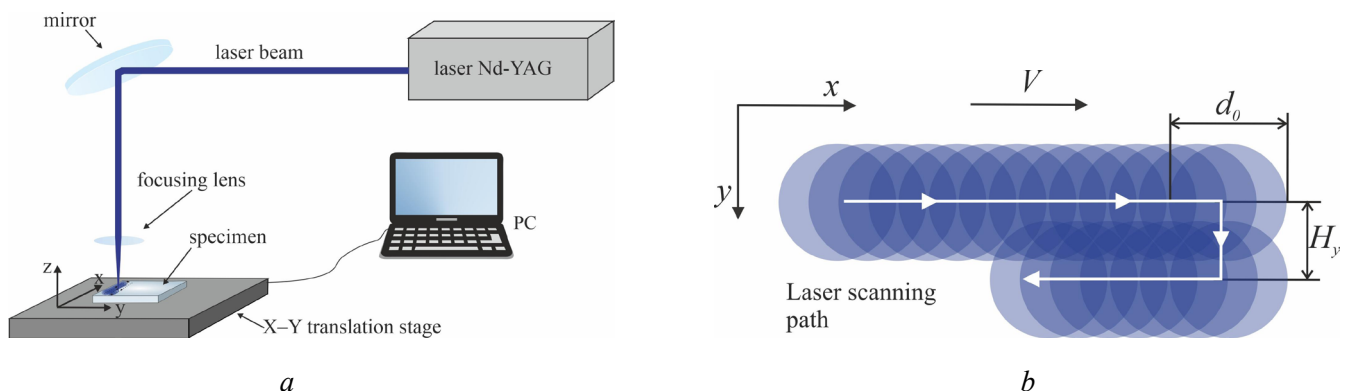


Fig. 1. Schematic of the experimental setup for *UV* laser surface treatment (a) and the scanning strategy employed (b). Diagram (b) illustrates the laser spot diameter (d_0), hatch distance (H_y), and scanning speed (V)

X-ray diffraction (*XRD*) analysis was employed to investigate the changes in the structure and phase composition of the *TiNi* alloy resulting from the *UV* laser treatment under different regimes. Diffraction patterns were acquired using a *DRON "Burevestnik"* diffractometer (Russia). A copper anode (*CuKα* radiation, $\lambda = 1.5418 \text{ Å}$) was used as the X-ray source, and the measurements were performed over a 2Θ range from 30° to 100°. The lattice parameter (a) was determined by extrapolating the values of a_{hkl} calculated for each diffraction peak with indices (hkl), against the function $0.5(\cos^2\theta/\sin\theta + \cos^2\theta/\theta)$.

Scanning Electron Microscopy (*SEM*) was used to investigate the microstructure and elemental composition of the specimen surfaces before and after *UV* laser treatment. The studies were conducted using a *TESCAN VEGA 3* microscope (Czech Republic) equipped with an Energy Dispersive X-ray Spectrometer (*EDS*). For a statistical evaluation of the elemental composition, *EDS* analysis was performed on at least ten randomly selected areas for each specimen.

The wettability of the surfaces before and after *UV* laser treatment was assessed using the sessile drop method with liquids of known surface tension. Droplets with a volume of 3 μL were dispensed onto the specimen surfaces using an automatic micropipette. After deposition, the droplets were allowed to stabilize for 60 seconds, after which their images were captured using a *Levenhuk Discovery Artisan 1024* digital

microscope. The contact angle values were averaged from at least five independent measurements. To quantitatively evaluate the changes in the surface properties induced by the *UV* laser treatment, the free surface energy (γ_{total}) and its components were determined. The calculations were performed according to the *Owens-Wendt-Rabel-Kaelble (OWRK)* method [20, 21], which allows for the separate evaluation of the dispersive (γ_d) and polar (γ_p) components of the total surface energy.

Results and Discussion

Fig. 2, *a* shows an *SEM* image of the microstructure and the elemental composition of the initial *TiNi* alloy specimen. It can be seen that the structure of the *TiNi* alloy is predominantly homogeneous. The matrix (light area in Fig. 2, *a*) contains a small fraction ($\leq 5\%$) of secondary phase inclusions (dark particles in Fig. 2, *a*). The *EDS* results presented in Fig. 2, *a* indicate that, in addition to the main matrix components *Ti* and *Ni*, small amounts of the *TN-10* alloying elements, such as *Fe* and *Mo*, as well as minor concentrations of *C* and *O*, were detected. The dark inclusions consist primarily of *Ti* and *C*, with a small amount of *Ni*. The presence of *Ni* in the spectra is likely attributable to the matrix surrounding these particles. Based on the elemental analysis, the light matrix corresponds to titanium nickelide (*TiNi*), while the dark inclusions are titanium carbide (*TiC*). This is further corroborated by the *XRD* data. The diffraction peaks in the *XRD* pattern obtained from the surface of the initial specimen, presented in Fig. 2, *b*, are identified as belonging to the *B2*-phase of *TiNi*. A peak attributed to *TiC* is also registered in the low-angle region. The lattice parameter of the *B2*-phase in the initial state was determined to be $a = 0.3018 \pm 0.0004$ nm.

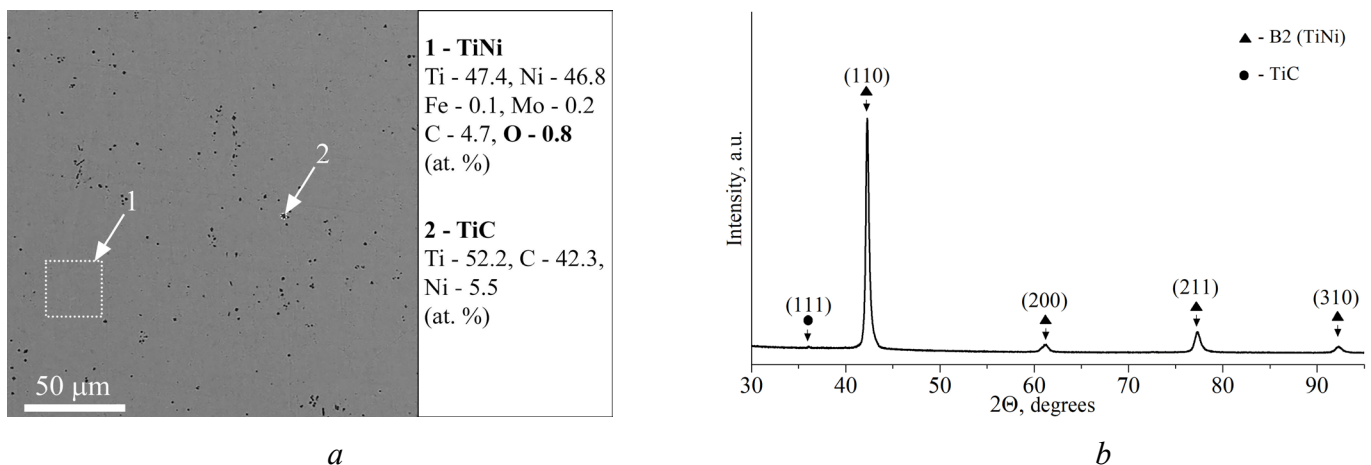


Fig. 2. Microstructural and compositional characterization of the untreated *TiNi* specimen surface:

(*a*) *SEM* micrograph with corresponding *EDS* elemental mapping; (*b*) X-ray diffraction pattern

The investigation of the structure, elemental, and phase composition of the *TiNi* alloy after *UV* laser treatment revealed that variations in laser processing parameters, such as wavelength and scanning speed, induce significant changes in the morphology, elemental, and phase composition of the surface layer.

Fig. 3 presents *SEM* images and the corresponding elemental composition of the *TiNi* alloy surface following *UV* laser treatment at wavelengths of 355 nm (Fig. 3, *a, c*) and 266 nm (Fig. 3, *b, d*), with laser scanning speeds of 500 $\mu\text{m/s}$ (Fig. 3, *a, b*) and 200 $\mu\text{m/s}$ (Fig. 3, *c, d*), respectively.

Fig. 3 reveals that after *UV* laser treatment at wavelengths of 355 nm and 266 nm with a scanning speed of 500 $\mu\text{m/s}$, the surface morphology of the material remains largely unchanged (Fig. 3, *a, b*). However, isolated microcracks are observed on the *TiNi* surface after treatment with the 266 nm wavelength, as indicated by the yellow arrows in Fig. 3, *b*. While the elemental composition of the *TiNi* surface remains the same after these treatment regimes, the quantitative ratios of the elements change. A comparison of the oxygen content on the initial and laser-modified surfaces showed that the amount of oxygen increases by 5–8 times after *UV* laser irradiation. Furthermore, the oxygen content on the *TiNi* surface is approximately 1.5 times higher after treatment with the shorter wavelength (266 nm) compared to the 355 nm wavelength.

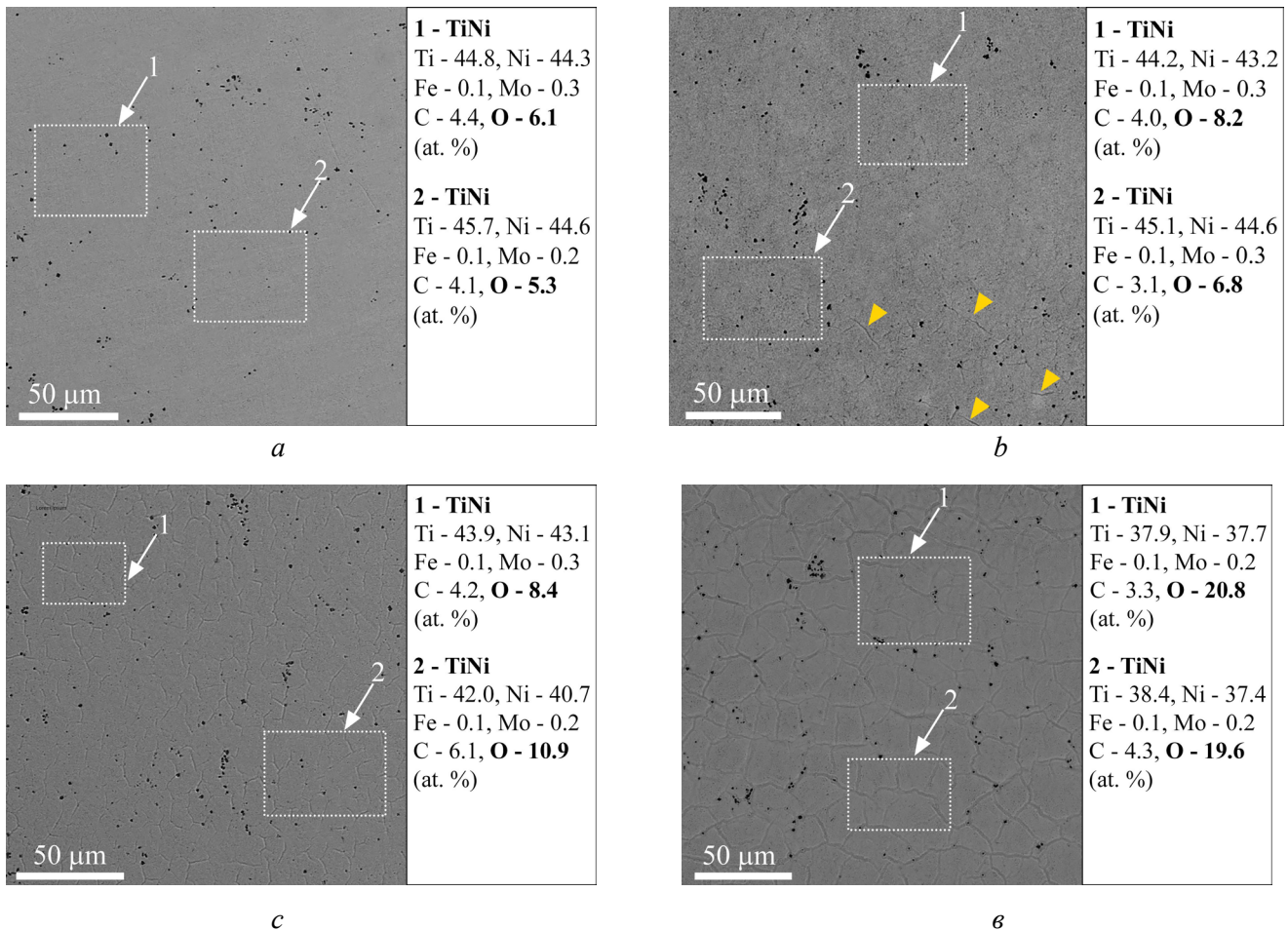


Fig. 3. SEM images of the *TiNi* alloy surface after *UV* laser treatment with different parameters and corresponding *EDS* analysis results:

(a) $\lambda = 355$ nm, $V = 500$ $\mu\text{m/s}$; (b) $\lambda = 266$ nm, $V = 500$ $\mu\text{m/s}$; (c) $\lambda = 355$ nm, $V = 200$ $\mu\text{m/s}$; (d) $\lambda = 266$ nm, $V = 200$ $\mu\text{m/s}$. (λ is a wavelength, V is a scanning speed)

As seen in Figs. 3, c and d, at the minimum scanning speed of 200 $\mu\text{m/s}$, a uniform network of microcracks is formed on the *TiNi* alloy surface under *UV* laser irradiation, regardless of the wavelength. The microcracking is more pronounced on the surface of specimens treated with the 266 nm wavelength at 200 $\mu\text{m/s}$. The formation of individual microcracks and the enhanced microcracking of the thin surface layer after *UV* laser treatment are attributed to several primary reasons related to the physical and chemical interaction of the laser radiation with the material.

The high energy of *UV* laser radiation causes rapid and localized surface heating, leading to abrupt thermal expansion and the subsequent development of significant thermal stresses within the material surface. The ultraviolet wavelength (100–400 nm) has a lower penetration depth into the material compared to *IR* or visible laser radiation. This concentrates the energy within a thin surface layer and increases the temperature gradient between the surface and the bulk material. Such a gradient amplifies internal stresses and promotes microcrack formation. The difference in the coefficients of linear thermal expansion between the underlying *TiNi* material and the metal oxides formed on the alloy surface during laser treatment may also contribute to microcracking [17, 22].

The scanning speed also influences the cracking process: a lower speed results in more intensive, prolonged exposure to a local area, which enhances the thermal load and the risk of crack formation. According to *EDS* data (Fig. 3), a significant increase in oxygen concentration, up to a depth of 3 μm , occurs under *UV* laser irradiation, depending on the wavelength. Whereas the initial (untreated) *TiNi* surface exhibited a minor oxygen content not exceeding 1 at.%, the surfaces treated with a 355 nm wavelength showed oxygen contents of 5.7 ± 0.4 at.% at a scanning speed of $V = 500$ $\mu\text{m/s}$ and 9.7 ± 1.3 at.% at

$V = 200 \text{ } \mu\text{m/s}$. For specimens treated with a 266 nm wavelength, an even more substantial increase in oxygen was observed: $7.5 \pm 0.7 \text{ at.}\%$ at $500 \text{ } \mu\text{m/s}$ and $18.7 \pm 2.1 \text{ at.}\%$ at $200 \text{ } \mu\text{m/s}$. The increased oxygen concentration on the *TiNi* alloy surface after laser treatment is likely caused by the intense interaction of *Ti* with atmospheric oxygen, leading to the formation of titanium oxides. The local thermal impact on the surface during laser treatment can result in the formation of oxide phases such as *TiO*, *TiO₂*, *Ti₂O₃*, and *Ti₂Ni₄O_x*. These phases not only enhance surface hardness and corrosion resistance but also improve surface hydrophilicity and bioactivity [17, 23, 24].

Fig. 4 presents the *XRD* patterns of *TiNi* specimens after *UV* laser treatment at a scanning speed of $200 \text{ } \mu\text{m/s}$. The *XRD* pattern obtained after *UV* laser treatment with a wavelength of 266 nm and a scanning speed of $200 \text{ } \mu\text{m/s}$ reveals, in addition to the primary *B2-TiNi* phase and traces of the secondary phase *TiC*, distinct peaks corresponding to titanium dioxide (*TiO₂*, rutile) and the complex oxide *Ni₂Ti₄O_x*. Therefore, the *XRD* data provide clear evidence of the formation of an oxide film on the *TiNi* alloy surface following *UV* laser treatment with a wavelength of 266 nm. In contrast, the *XRD* patterns of *TiNi* specimens irradiated with a 355 nm wavelength, even at the lowest scanning speed of $200 \text{ } \mu\text{m/s}$, show only peaks belonging to the *B2-TiNi* phase and the *TiC* impurity phase. The absence of diffraction peaks from oxide phases on the *XRD* patterns obtained after irradiation with the 355 nm wavelength could be attributed to either a very thin oxide film, a low concentration of oxides (less than 3%) below the detection limit of the *XRD* technique, or the potential quasi-amorphous nature of the oxide phases. This quasi-amorphous state could prevent the identification of oxides on the laser-modified surface under these specific *UV* laser treatment parameters using the *XRD* method. The lattice parameter of the *B2*-phase in the *TiNi* specimens subjected to *UV* laser treatment decreased compared to the initial state: to $a = 0.3016 \pm 0.0002 \text{ nm}$ for $\lambda = 355 \text{ nm}$ ($V = 200 \text{ } \mu\text{m/s}$) and to $a = 0.3014 \pm 0.0001 \text{ nm}$ for $\lambda = 266 \text{ nm}$. This reduction in the lattice parameter may qualitatively indicate a depletion of titanium in the *B2-TiNi* matrix and an associated change in the phase composition of the specimens.

The changes in the morphology, elemental, and phase composition of the *TiNi* alloy surface induced by pulsed *UV* laser treatment significantly affect its surface properties, such as wettability and free surface energy.

The wettability of titanium nickelide (*TiNi*) plays a crucial role in the material's biocompatibility, influencing cell proliferation on its surface. As shown in [25], a moderately hydrophilic surface on *TiNi* implants, with a water contact angle of less than 60° , ensures good wetting by biological fluids and enhanced

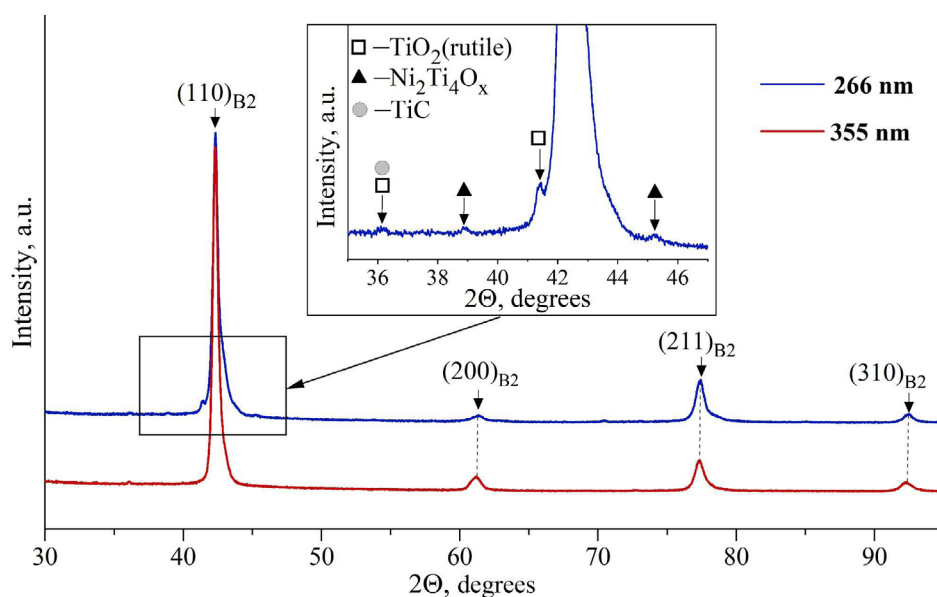


Fig. 4. X-ray diffraction (*XRD*) patterns obtained from *TiNi* specimens after *UV* laser treatment at wavelengths of $\lambda = 266 \text{ nm}$ and $\lambda = 355 \text{ nm}$, using a scanning speed of $200 \text{ } \mu\text{m/s}$

cell adhesion, thereby stimulating the proliferation of endothelial and smooth muscle cells. Increased hydrophilicity promotes more active cell adhesion, spreading, and multiplication, which is particularly important for medical implants. The degree of hydrophilicity, characterized by the material surface's ability to attract and hold water, is determined by the water contact angle.

UV laser treatment of the *TiNi* alloy surface alters its hydrophilicity. The average water contact angle for the initial *TiNi* specimens was $75.1^\circ \pm 3.8^\circ$. After *UV* laser treatment, the hydrophilicity increases substantially. The plots of the water contact angle versus scanning speed for the *TiNi* alloy surface treated with *UV* laser radiation at wavelengths of 266 nm and 355 nm are presented in Fig. 5. Representative images of water droplets on the *UV* laser-treated surfaces are provided in the insets of Fig. 5. A decrease in the laser wavelength and a reduction in the scanning speed during *UV* laser treatment lead to a decrease in the contact angle. As shown by the data presented in Fig. 5, when the material is laser treated with a 355 nm wavelength at the maximum scanning speed of 5,000 $\mu\text{m/s}$, the contact angle decreases by 10% compared to the initial state. When the scanning speed is reduced to 200 $\mu\text{m/s}$, the contact angle decreases threefold to $24.7^\circ \pm 1.5^\circ$. The most pronounced increase in hydrophilicity is observed after *UV* laser treatment with a wavelength of 266 nm. Even at the maximum scanning speed (5,000 $\mu\text{m/s}$), the contact angle is reduced by more than threefold compared to the initial state. It should be noted that reducing the scanning speed from 5,000 $\mu\text{m/s}$ to 200 $\mu\text{m/s}$ has only a minor effect on surface hydrophilicity at this wavelength, with the contact angle varying within the range of 11–20°.

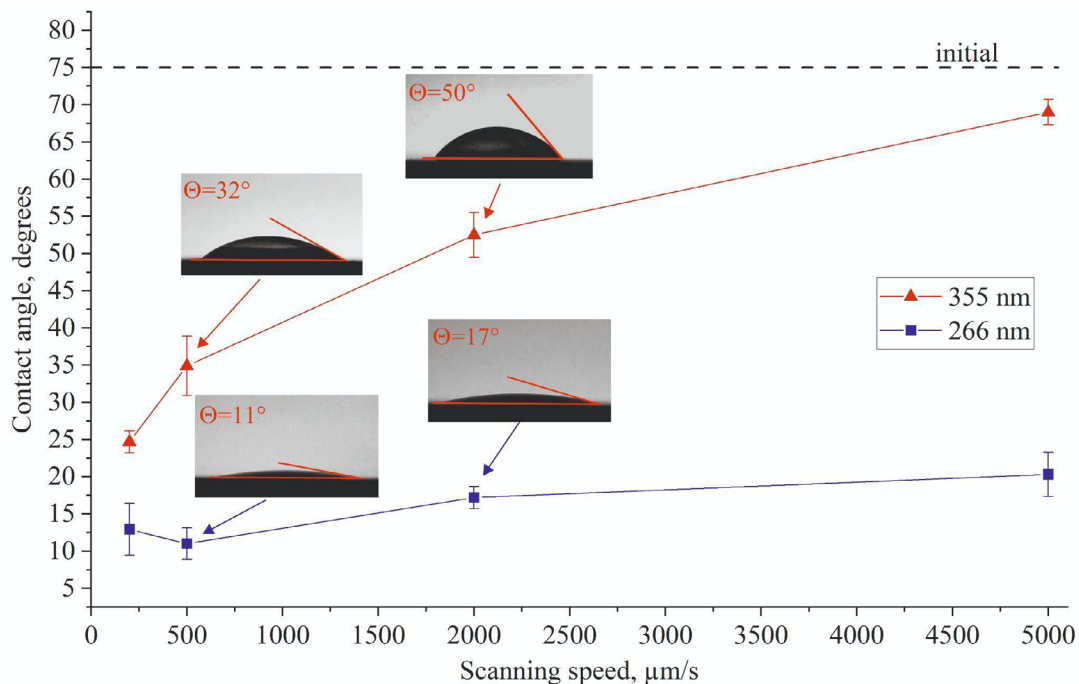


Fig. 5. Effect of laser wavelength on the dependence of the water contact angle on the scanning speed during *UV* laser treatment

Surface hydrophilicity is directly related to the magnitude of the free surface energy. An increase in free surface energy, achieved through surface modification techniques such as *UV* laser treatment or the application of hydrophilic coatings, leads to enhanced wettability. This, in turn, improves functional characteristics such as adhesion, biocompatibility, and cell proliferation [26, 27]. Fig. 6 shows the dependencies of the free surface energy and its components on the wavelength of *UV* laser radiation and the scanning speed during surface treatment of *TiNi* specimens.

Following *UV* laser treatment, the ratio between the dispersive (γ_d) and polar (γ_p) components of the surface energy changes. A more than two-fold decrease in the dispersive component and a significant increase in the polar component are observed.

When the scanning speed is reduced during *UV* laser treatment, the value of the dispersive component remains almost unchanged and does not exceed 10 mJ/m^2 , while the polar component increases by 5 to 7

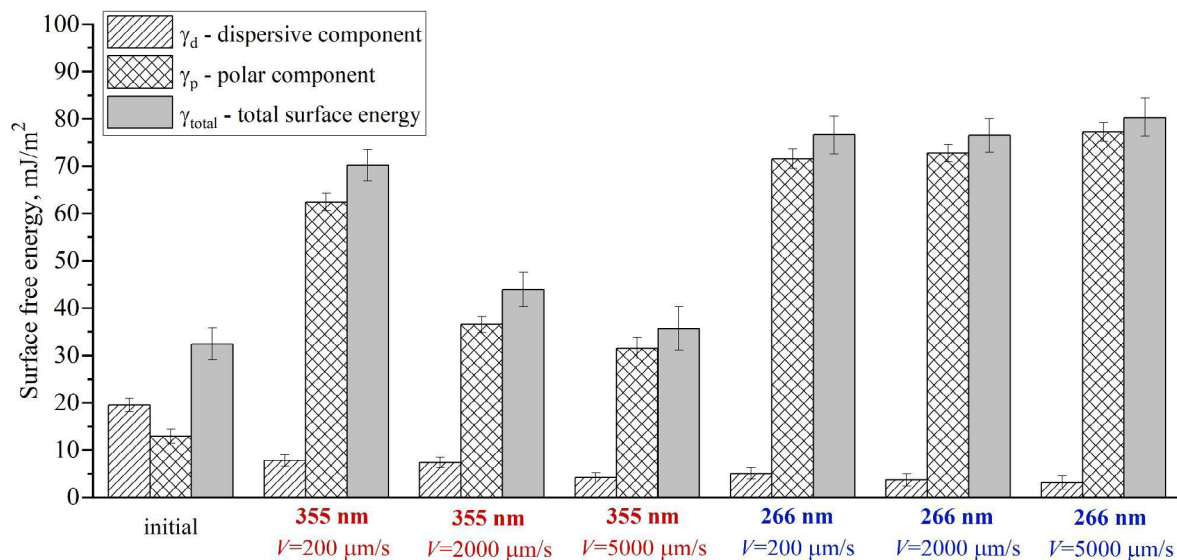


Fig. 6. Surface free energy (γ_{total}) and its components (polar γ_p and dispersive γ_d) of *TiNi* specimens before and after *UV* laser treatment with different parameters

times. This effect is primarily attributed to the oxidation of the *TiNi* surface during laser treatment, which increases the oxygen content and leads to the formation of polar oxide groups. These groups enhance the polar component of the surface energy, thereby increasing the material's hydrophilicity. In addition, it can be assumed that during *UV* laser treatment, the surface electric potential of *TiNi* specimens shifts to the positive region. As a result, surfactant molecules from the environment adsorb onto the modified surface in such a way that their hydrophilic polar groups, which carry a positive charge, are oriented away from the surface, while the hydrocarbon radicals, which exhibit hydrophobic properties, are directed towards the metal. It is this reorientation of the adsorbed layer that can explain the sharp increase in the polar component of the surface energy [28].

A comparative analysis of the laser treatment modes revealed distinct differences in the effects of *UV* laser radiation at 266 nm and 355 nm wavelengths on the *TiNi* specimens. For the 355 nm wavelength, the free surface energy exhibits a dependence on the scanning speed: as the speed decreases, the surface energy increases. In contrast, the surface treated with the 266 nm wavelength demonstrates different behavior. Even at the maximum scanning speed ($V = 5000 \mu\text{m/s}$), the surface energy increases approximately 2 times compared to the initial state. A further reduction in the scanning speed results in only minor changes to the free surface energy and its components (γ_d and γ_p). These results are consistent with the water contact angle measurements presented in Fig. 5.

The different effects of 266 nm and 355 nm *UV* laser surface treatment on the water contact angle of *TiNi* specimens are caused by the distinct changes in the free surface energy, which depends on both the microrelief and the structural-chemical characteristics of the surface formed after *UV* laser treatment. Key governing parameters that determine surface modification during laser treatment include wavelength, pulse energy, pulse repetition rate, pulse duration, and the spatial beam profile. In the present case, the wavelength was the variable parameter. Therefore, the observed difference in the structure and properties of the surface after modification with 266 nm and 355 nm radiation is specifically related to the distinct influence of the laser wavelength.

The difference in the characteristics of the *TiNi* specimen surfaces modified by ultraviolet laser radiation with wavelengths of 266 nm and 355 nm is primarily due to the distinct degree of interaction between the radiation and the material. This is related to the differences in reflectivity and the material's absorption coefficient at these wavelengths. *UV* laser radiation with a wavelength of 266 nm possesses higher photon energy and exhibits significantly greater energy absorption within the surface layer of the material. This leads to more intense local heating and surface oxidation. In turn, *UV* laser radiation with a wavelength of 355 nm is characterized by a greater penetration depth, resulting in a different energy distribution and

the formation of a distinct surface microstructure. The experimentally determined values of the reflection coefficient R , measured using a *Gentec QE50LP-H-MB-D0* energy meter, were $R \approx 20\%$ for the 266 nm wavelength and $R \approx 30\%$ for 355 nm. These data are in good agreement with the results obtained for the *Ti6Al4V* alloy [16], where it was established that the reflectivity of the alloy increases with the wavelength of the incident laser radiation in the range of 266 to 1064 nm. The lower value of the reflection coefficient for *UV* laser radiation with a wavelength of 266 nm indicates significantly greater energy absorption in the near-surface layer, which is explained by the higher photon energy. Consequently, these differences affect the changes in morphology, chemical composition, phase state of the surface, as well as the free surface energy and hydrophilicity of the material after *UV* laser treatment. Therefore, *UV* laser radiation with a wavelength of 266 nm is characterized by a lower penetration depth and a more intense effect on the surface layers, which determines the differences in the resulting microstructure and chemical composition of the *TiNi* specimens after *UV* laser treatment.

Conclusion

1. It was established that at scanning speeds above 500 $\mu\text{m/s}$, the original surface morphology of the *TiNi* alloy is preserved upon exposure to *UV* laser radiation at wavelengths of 266 and 355 nm. The formation of isolated microcracks is observed on the *TiNi* alloy surface subjected to *UV* laser radiation at a scanning speed of $V = 500 \mu\text{m/s}$ only with the 266 nm wavelength. At the lowest scanning speed of $V = 200 \mu\text{m/s}$, exposure to *UV* laser radiation for both wavelengths (266 and 355 nm) leads to the formation of localized structural damage on the *TiNi* alloy surface in the form of a microcrack network. The individual microcracks and the overall microcracking of the *TiNi* surface after *UV* treatment are caused by local thermal stresses arising from rapid heating and subsequent quenching of the surface during the *UV* laser treatment.

2. It was demonstrated that during *UV* laser treatment of the *TiNi* alloy surface, a decrease in the radiation wavelength from 355 to 266 nm and a reduction in scanning speed from 5,000 to 200 $\mu\text{m/s}$ lead to an increase in oxygen content in the near-surface layer of *TiNi* up to $\approx 20 \text{ at.}\%$ ($\lambda = 266 \text{ nm}$, $V = 200 \mu\text{m/s}$) and $\approx 10 \text{ at.}\%$ ($\lambda = 355 \text{ nm}$, $V = 200 \mu\text{m/s}$), with the formation of titanium oxides.

3. *UV* laser treatment results in a significant increase in the wettability of the *TiNi* surface. The maximum reduction in the water contact angle to $\approx 11^\circ$ was achieved using radiation with a wavelength of 266 nm, whereas treatment with 355 nm laser radiation reduced the angle to $\approx 25^\circ$ ($V = 200 \mu\text{m/s}$). It was determined that the observed significant increase in the hydrophilicity of the *TiNi* specimens is due to the enrichment of the near-surface layer with oxygen, the formation of oxide phases, and, consequently, a substantial increase in the free surface energy driven by a sharp rise in its polar component.

Thus, *UV* laser treatment with a wavelength of 266 nm induces more significant changes in the morphology and properties of the *TiNi* alloy surface compared to 355 nm radiation under identical processing regimes. This is manifested in more intense surface oxidation with the formation of oxide phases, more pronounced development of microcracks at low scanning speeds (200 and 500 $\mu\text{m/s}$), and a substantial enhancement of hydrophilicity. The observed effects are associated with the higher photon energy and the lower surface reflection coefficient ($R \approx 20\%$ for 266 nm radiation versus $R \approx 30\%$ for 355 nm radiation) of the *TiNi* specimens. This ensures efficient energy absorption in the near-surface layer and promotes changes in morphology and topography, as well as oxidation processes on the surface of the *TiNi* specimens.

References

1. Jani J.M., Leary M., Subic A., Gibson M.A. A review of shape memory alloy research, applications and opportunities. *Materials & Design*, 2014, vol. 56, pp. 1078–1113. DOI: 10.1016/j.matdes.2013.11.084.
2. Elahinia M., Moghaddam N.S., Andani M.T., Amerinatanzi A., Bimber B.A., Hamilton R.F. Fabrication of NiTi through additive manufacturing: A review. *Progress in Materials Science*, 2016, vol. 83, pp. 630–663. DOI: 10.1016/j.pmatsci.2016.08.001.
3. Ryhänen J., Kallioinen M., Tuukkanen J., Junila J., Niemelä E., Sandvik P., Serlo W. In vivo biocompatibility evaluation of nickel-titanium shape memory metal alloy: Muscle and perineural tissue responses and encapsule

membrane thickness. *Journal of Biomedical Materials Research*, 1998, vol. 41 (3), pp. 481–488. DOI: 10.1002/(sici)1097-4636(19980905)41:3<481::aid-jbm19>3.0.co;2-l.

4. Liu K., Yao X., Jiang L. Recent developments in bio-inspired special wettability. *Chemical Society Reviews*, 2010, vol. 39 (8), pp. 3240–3255. DOI: 10.1039/b917112f.

5. Poon R.W.Y., Ho J.P.Y., Liu X., Chung C.Y., Chu P.K., Yeung K.W.K., Lu W.W., Cheung K.M.C. Improvements of anti-corrosion and mechanical properties of NiTi orthopedic materials by acetylene, nitrogen and oxygen plasma immersion ion implantation. *Nuclear Instruments and Methods in Physics Research, Section B: Beam Interactions with Materials and Atoms*, 2005, vol. 237 (1–2), pp. 411–416. DOI: 10.1016/j.nimb.2005.05.030.

6. Slobodyan M.S., Markov A.B. Laser and electron-beam surface processing on TiNi shape memory alloys: a review. *Russian Physics Journal*, 2024, vol. 67 (5), pp. 565–615. DOI: 10.1007/s11182-024-03158-5.

7. Meisner L.L., Markov A.B., Rotshtein V.P., Ozur G.E., Meisner S.N., Yakovlev E.V., Semin V.O., Mironov Yu.P., Poletika T.M., Girsova S.L., Shepel D.A. Microstructural characterization of Ti-Ta-based surface alloy fabricated on TiNi SMA by additive pulsed electron-beam melting of film/substrate system. *Journal of Alloys and Compounds*, 2018, vol. 730, pp. 376–385. DOI: 10.1016/j.jallcom.2017.09.238.

8. Firstov G.S., Vitchev R.G., Kumar H., Blanpain B., Van Humbeeck J. Surface oxidation of NiTi shape memory alloy. *Biomaterials*, 2002, vol. 23 (24), pp. 4863–4871. DOI: 10.1016/S0142-9612(02)00244-2.

9. Marchenko E., Yasenchuk Yu., Baigonakova G., Gunther S., Yuzhakov M., Zenkin S., Potekaev A., Dubovikov K. Phase formation during air annealing of Ti-Ni-Ti laminate. *Surface and Coatings Technology*, 2020, vol. 388, p. 125543. DOI: 10.1016/j.surfcoat.2020.125543.

10. Khan M.A., Halil A.M., Abidin M.S.Z., Hassan M.H., Rahman A.A.A. Influence of laser surface texturing on the surface morphology and wettability of metals and non-metals: A review. *Materials Today Chemistry*, 2024, vol. 41, p. 102316. DOI: 10.1016/j.mtchem.2024.102316.

11. Pequegnat A., Michael A., Wang J., Lian K., Zhou Y., Khan M.I. Surface characterizations of laser modified biomedical grade NiTi shape memory alloys. *Materials Science and Engineering: C*, 2015, vol. 50, pp. 367–378. DOI: 10.1016/j.msec.2015.01.085.

12. Zhang Q., Dong J., Peng M., Yang Z., Wan Y., Yao F., Zhou J., Ouyang C., Deng X., Luo H. Laser-induced wettability gradient surface on NiTi alloy for improved hemocompatibility and flow resistance. *Materials Science and Engineering: C*, 2020, vol. 111, p. 110847. DOI: 10.1016/j.msec.2020.110847.

13. Biffi C.A., Fiocchi J., Rancan M., Gambaro S., Cirisano F., Armelao L., Tuissi A. Ultrashort laser texturing of superelastic NiTi: Effect of laser power and scanning speed on surface morphology, composition and wettability. *Metals*, 2023, vol. 13 (2), p. 381. DOI: 10.3390/met13020381.

14. Chan C.-W., Carson L., Smith G.C. Fibre laser treatment of martensitic NiTi alloys for load-bearing implant applications: Effects of surface chemistry on inhibiting *Staphylococcus aureus* biofilm formation. *Surface and Coatings Technology*, 2018, vol. 349, pp. 488–502. DOI: 10.1016/j.surfcoat.2018.06.015.

15. Chenrayan V., Vaishnav V., Shahapurkar K., Dhanabal P., Kalayarasan M., Raghunath S., Mano M. The effect of fs-laser micromachining parameters on surface roughness, bio-corrosion and biocompatibility of nitinol. *Optics & Laser Technology*, 2024, vol. 170, p. 110200. DOI: 10.1016/j.optlastec.2023.110200.

16. Milovanović D.S., Radak B.B., Gaković B.M., Batani D., Momčilović M.D., Trtica M.S. Surface morphology modifications of titanium based implant induced by 40 picosecond laser pulses at 266 nm. *Journal of Alloys and Compounds*, 2010, vol. 501 (1), pp. 89–92. DOI: 10.1016/j.jallcom.2010.04.047.

17. Sablina T.Y., Panchenko M.Yu., Zyatikov I.A., Puchikin A.V., Konovalov I.N., Panchenko Yu.N. Study of surface hydrophilicity of metallic materials modified by ultraviolet laser radiation. *Obrabotka metallov (tekhnologiya, oborudovanie, instrumenty) = Metal Working and Material Science*, 2024, vol. 26, no. 4, pp. 218–233. DOI: 10.17212/1994-6309-2024-26.4-218-233. (In Russian).

18. Wang Y., Zhang M., Li K., Hu J. Study on the surface properties and biocompatibility of nanosecond laser patterned titanium alloy. *Optics & Laser Technology*, 2021, vol. 139, p. 106987. DOI: 10.1016/j.optlastec.2021.106987.

19. Li S., Cui Z., Zhang W., Li Y., Li L., Gong D. Biocompatibility of micro/nanostructures nitinol surface via nanosecond laser circularly scanning. *Materials Letters*, 2019, vol. 255, p. 126591. DOI: 10.1016/j.matlet.2019.126591.

20. Hebbar R.S., Isloor A.M., Ismail A.F. Contact angle measurements. *Membrane Characterization*. Ed. by N. Hilal, A.F. Ismail, T. Matsuura, D. Oatley-Radcliffe. Elsevier, 2017, pp. 219–255. DOI: 10.1016/B978-0-444-63776-5.00012-7.

21. Owens D.K., Wendt R.C. Estimation of the surface free energy of polymers. *Journal of Applied Polymer Science*, 1969, vol. 13 (8), pp. 1741–1747. DOI: 10.1002/app.1969.070130815.



22. Razi S., Mollabashi M., Madanipour K. Laser processing of metallic biomaterials: An approach for surface patterning and wettability control. *The European Physical Journal Plus*, 2015, vol. 130, p. 247. DOI: 10.1140/epjp/i2015-15247-5.
23. Min J., Wan H., Carlson B.E., Lin J., Sun C. Application of laser ablation in adhesive bonding of metallic materials: A review. *Optics & Laser Technology*, 2020, vol. 128, p. 106188. DOI: 10.1016/j.optlastec.2020.106188.
24. Choi H., Na M., Jun I., Lee M.-H., Jung H.-D., Lee H., Han J., Lee K., Park C.-H., Kim H.-E., Song J., Koh Y.-H., Kim S. Repetitive nanosecond laser-induced oxidation and phase transformation in NiTi alloy. *Metals and Materials International*, 2024, vol. 30, pp. 1200–1208. DOI: 10.1007/s12540-023-01581-w.
25. Yasenchuk Yu.F., Gunther S.V., Kokorev O.V., Marchenko E.S., Gunther V., Baigonakova G.A., Dubovikov K.M. The influence of surface treatment on wettability of TiNi-based alloy. *Russian Physics Journal*, 2019, vol. 62 (2), pp. 333–338. DOI: 10.1007/s11182-019-01716-w.
26. Villapun Puzas V.M., Carter L.N., Schröder C., Colavita P.E., Hoey D.A., Webber M.A., Addison O., Shepherd D.E.T., Attallah M.M., Grover L.M., Cox S.C. Surface free energy dominates the biological interactions of postprocessed additively manufactured Ti-6Al-4V. *ACS Biomaterials Science & Engineering*, 2022, vol. 8 (10), pp. 4311–4326. DOI: 10.1021/acsbiomaterials.2c00298.
27. Peethan A., Unnikrishnan V.K., Chidangil S., George S.D. Laser-assisted tailoring of surface wettability – Fundamentals and applications: A critical review. *Progress in Adhesion and Adhesives*. Vol. 5. *Surface modification of polymers: methods and applications*. Ed. by K.L. Mittal, S.D. George. Scrivener Publishing LLC, 2020, pp. 331–265. ISBN 9781119748069. DOI: 10.1002/9781119749882.ch11.
28. Ryzhenkov A.V., Volkov A.V., Trushin E.S., Cherepanov S.P. Change of wettability of stainless steel surface based on laser texturing of relief. *Global'naya energiya = Global Energy*, 2022, vol. 28, no. 4, pp. 136–146. DOI: 10.18721/JEST.28409. (In Russian).

Conflicts of Interest

The authors declare no conflict of interest.

© 2025 The Authors. Published by Novosibirsk State Technical University. This is an open access article under the CC BY license (<http://creativecommons.org/licenses/by/4.0>).

